

Threshold measurements of the *K*-shell photoelectron satellites in Ne and Ar

P. H. Kobrin,* S. Southworth,[†] C. M. Truesdale,[‡] D. W. Lindle, U. Becker,[§] and D. A. Shirley

Materials and Molecular Research Division, Lawrence Berkeley Laboratory, University of California, Berkeley, California 94720
and Department of Chemistry, University of California, Berkeley, California 94720

(Received 31 May 1983)

The relative intensities of *K*-shell photoelectron satellites near their respective thresholds in Ne and Ar have been measured using synchrotron radiation. The Ne satellites were found to be 25–40% smaller than in the high-energy limit. The $2p \rightarrow 3s$ “conjugate shakeup” state of Ne^+ was not observed, in contrast to predictions of many-body perturbation theory. The asymmetry parameter of the neon Auger group was found to be equal to zero at the $1s \rightarrow 3p$ resonance at 867 eV. This result may indicate that the $3p$ Rydberg electron is essentially decoupled from the core in the Auger decay process. In argon, a *K*-shell satellite was observed at 24.6(3) eV with 6% intensity relative to the main line, confirming a theoretical prediction by Dyall. Tentative evidence was obtained that this branching ratio increases with energy in the first 90 eV above threshold.

I. INTRODUCTION

Inner-shell photoelectron spectra of closed-shell atoms typically show an intense peak at the binding energy of each electronic subshell, and weaker “satellite peaks” at higher binding energies. The satellites arise via photoionization to higher-energy states of the ion, which are approximately described by configurations formed by the removal of a core electron and the promotion of a valence electron to a higher subshell. Thus, for example, the main peak in a Ne $1s$ photoionization spectrum would correspond to the $\text{Ne}^+(1s2s^22p^6)$ state, whereas a typical satellite configuration would be $\text{Ne}^+(1s2s^22p^53p)$. Because the presence of satellites cannot be explained in an independent-particle description of the atom, but rather require a many-electron picture, they are known as “correlation satellites.” The study of these satellites is important for an understanding of the many-particle nature of atomic structure and the photoionization process.

A heuristic approach to correlation satellites is the “shake” theory,¹ in which the above description is used to estimate satellite intensities by projecting the passive orbitals of the neutral atom onto those of the ion, in which these orbitals have relaxed in response to the new atomic potential. This procedure is best suited to phenomena well above the satellite threshold and is implicitly limited to a one-configuration description of each state.

A more general approach to correlation satellites, capable of extension to the energy range closer to threshold, is an explicit treatment of electron correlation with methods based on configuration interaction (CI). In this framework the equivalence of photoionization channels leading to the “main” ionic final state and the “satellite” states is explicitly recognized, as is the equivalence of these states as eigenstates of the $(N-1)$ -electron Hamiltonian, independent of any reference to photoemission.^{2,3} Three different CI mechanisms that contribute to satellite intensities have been classified: initial-state configuration interaction (ISCI) and final-ionic-state configuration interaction

(FISCI), which are photon-energy independent; and continuum-state configuration interaction (CSCI), which is highly energy dependent and more important near threshold. Many calculations have been made of satellite intensities in the high-energy, or sudden, limit where CSCI effects are less important.^{3–9} For the Ne $1s$ correlation satellites, Martin and Shirley⁹ have shown that both ISCI and FISCI are required to obtain good agreement with the experimental intensities observed at high energy.

Far less is known about the energy dependence of satellite intensities.^{10–12} In the photoionization of helium, the relative intensity (the satellite-to-main-line ratio) of the $2s$ state was found^{13,14} to be constant up to 60 eV above threshold, while the relative intensity of the $2p$ state decreased by a factor of 3. The He $2s$ state is referred to as a “shakeup” satellite, because it differs from the main line by a $1s \rightarrow 2s$ excitation. The $2p$ state is referred to as a “conjugate shakeup” satellite, because it differs from the main line by a $1s \rightarrow 2p$ excitation and a consequent change in parity. Configuration interaction in the continuum is more important for conjugate shakeup satellites, and they are therefore more energy dependent. For the neon $2s$ and $2p$ shakeup states, the relative intensities near threshold were found to be less than half of their high-energy values.¹⁰ Also, the relative intensities of the Ne $2s$ satellites (referred to the $2s$ main line) reach maximum values at intermediate energies.

Except for the special case of the He^+ ($n=2$) satellites, the only energy-dependent calculations to date have been on Li,¹⁵ Fe,¹⁶ and on the $2p \rightarrow 3s$ satellite in the Ne *K*-shell spectrum. Ishihara, Mizuno, and Watanabe¹⁷ have used many-body perturbation theory (MBPT) to model the continuum processes that give intensity to this Ne conjugate shakeup peak. Their calculated relative intensity of 0.1% at 600-eV kinetic energy is in good agreement with the $\text{AlK}\alpha$ measurement.¹⁸ They also predict that the satellite intensity should increase to almost 5% of the intensity of the main line near threshold. The MBPT calculation, however, was performed only in lowest order and only in

the dipole length form.

With the advent of the availability of high-energy synchrotron radiation, it is now becoming feasible to study correlation satellites near core-level thresholds, thereby addressing these more subtle questions concerning the energy dependences of satellite intensities. We present in this report the first such measurements for *K*-shell satellites of neon (*K*-shell binding energy is 870.4 eV) and argon (*K*-shell binding energy is 3206 eV). The experimental procedures are described in Sec. II and results are given in Sec. III.

II. EXPERIMENTAL

Radiation from the electron storage ring SPEAR at the Stanford Synchrotron Radiation Laboratory was monochromatized by JUMBO, a constant-deviation double-crystal monochromator on beam line III-2.¹⁹ The storage ring was operated in the parasitic mode at 6–12 mA and 1.85 GeV so that the photon flux was an order of magnitude lower than during high-energy dedicated operation. The photon flux was higher for the Ar spectra taken between 3210 and 3320 eV ($\sim 10^{10}$ photons per second) than for the Ne spectra taken between 860 and 960 eV ($\sim 10^9$ photons per second). The monochromator bandpass [full width at half maximum (FWHM)] was ~ 0.75 eV for the Ne spectra and ~ 1.7 eV for the Ar spectra. Count rates for the satellite lines were low (0.1 – 0.2 sec⁻¹ in Ne and 0.2 – 0.6 sec⁻¹ in Ar), reflecting their low cross sections (0.01 Mb in Ne and 0.005 Mb in Ar). Despite this constraint, we obtained the highest-energy gas-phase photoelectron spectra ever recorded with synchrotron radiation by making use of the efficiency of time-of-flight (TOF) electron analysis.

Our TOF spectrometer has been described previously.²⁰ Each spectrum was accumulated for 30–100 min at a sample pressure of 1×10^{-3} Torr in the chamber, approximately 5×10^{-3} Torr in the interaction region and less than 3×10^{-5} Torr in the differentially pumped electron analyzers. A 1500-Å-thick vitreous carbon window ($> 95\%$ transmission in this photon-energy range) was used to isolate the spectrometer from the ultrahigh vacuum monochromator.

The electron-energy resolution was improved by retarding the photoelectrons over part of their flight path. The energy resolution of the TOF analyzer is approximately a fixed fraction (0.05 for this experiment) of the kinetic energy of the photoelectrons after retardation. The resolution was limited by the size of the horizontal focus (5 mm) on the JUMBO monochromator.

Two TOF analyzers were operated at angles of $\theta = 0^\circ$ and $\theta = 54.7^\circ$ with respect to the photon polarization direction. The intensity $I(\theta)$ of a given photoelectron peak produced by linearly-polarized light in the dipole approximation is given by

$$I(\theta) \propto \frac{d\sigma(\theta)}{d\Omega} = \frac{\sigma}{4\pi} [1 + \beta P_2(\cos\theta)],$$

where σ is the partial cross section and β is the angular distribution asymmetry parameter. Throughout this paper, we assume the validity of the dipole approximation,

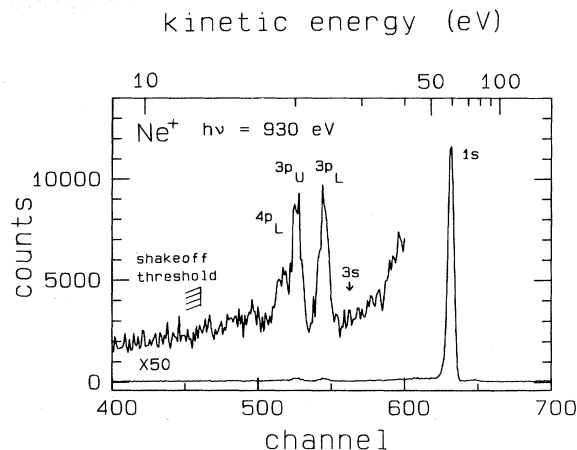


FIG. 1. Electron TOF spectrum of Ne. The accumulation time is 100 min, and there are 2.4 channels per nsec. The peak assignments are given in Table I. The $2p \rightarrow 3s$ conjugate shakeup satellite is not observed. Not shown is the *KLL* Auger peak at channel 736. The *K*-shell shakeoff threshold occurs at an excitation energy of 47.4 eV.

implying that β completely describes the angular distribution of photoelectrons.

For *K*-shell shakeup satellites, the satellite and the main line are expected to have $\beta = 2$. Because the 0° analyzer receives a factor of 3 more intensity for these lines, it was used for the branching-ratio measurements. Because the β values are equal, no angular correction to the intensity ratios should be necessary. For the Ne $2p \rightarrow 3s$ “conjugate shakeup” satellite, the β parameter may be different from 2.0, and branching-ratio measurements from the 0° analyzer must be corrected accordingly.

Using the TOF method, all electrons were accumulated simultaneously so that the observed branching ratios are independent of photon-flux and gas-pressure fluctuations. The analyzer transmission as a function of electron kinetic energy and retarding voltage was calibrated by comparing the intensity of the main Ne *1s* peak to the intensity of the *KLL* Auger peak. Any variations in this ratio are attributed to a varying analyzer transmission for the (much lower energy) *1s* peak.

Both analyzers are required to measure the β parameter.²¹ We used this double-angle time-of-flight (DATOF) method to measure the β parameter of the *KLL* Auger electrons in Ne above the *1s* threshold and the corresponding autoionization electrons at the $1s \rightarrow 3p$ resonance below threshold.

III. RESULTS

Gelius¹⁸ recorded a well-resolved spectrum of the Ne *K*-shell satellites using $AlK\alpha$ x rays ($h\nu = 1487$ eV), and assigned configuration states to the observed peaks. We adopt these assignments for the present spectra. Figure 1 shows a TOF spectrum of Ne taken at 930 eV, which is 23 eV above the threshold of the first shakeup satellite $3p_L$ (see Table I). In this spectrum the resolution in the energy

TABLE I. Summary of the neon *K*-shell peaks.

Line	Assignment	Excitation energy (eV) ^b	Relative intensity	
			930 eV	1487 eV ^b
1s	1s2s ² 2p ⁶ 2S	(870.4)	100	100
3s	1s2s ² 2p ⁵ 3s ² P	33.4	<0.9 ^c	0.06(1)
3p _L	1s2s ² 2p ⁵ 3p ² S (lower) ^a	37.4	2.5(2)	3.15(8)
3p _U	1s2s ² 2p ⁵ 3p ² S (upper) ^a	40.8	3.0(2)	3.13(10)
4p _L	1s2s ² 2p ⁵ 4p ² S (lower) ^a	42.3		2.02(10)

^aThe “lower” and “upper” notation is used to distinguish between two states with the same configuration (Ref. 9).

^bFrom Ref. 18.

^cCorrected for $\beta=0.7$.

region of the satellites is approximately 1.2 eV. No evidence of the $2p \rightarrow 3s$ conjugate shakeup peak is seen between the main line and the $3p_L$ line. The $3p_L$ peak is well resolved, while the $3p_U$ and $4p_L$ peaks are unresolved. Above the $4p_L$ satellite in binding energy, there are known to be several weaker, unresolved satellites that are not discernible in this spectrum.

The satellite intensities relative to the main line from several spectra are displayed in Fig. 2. The error bars include both counting statistics and the uncertainty in background subtraction. For the $3p_L$ satellite in Fig. 2(a), we find that the mean relative intensity is approximately 2.2(2)%, which is 25% below the value obtained by Gelius at 1487 eV.¹⁸ For the sum of the $3p_U$ and $4p_L$ satellites in Fig. 2(b), we obtain a relative intensity of 3.1(2)%, 40%

below the $AlK\alpha$ value.¹⁸ Although the data in both plots show fairly large errors and considerable scatter, the results in Fig. 2 appear roughly constant with energy.

The data represented in Fig. 2 are the first core-level satellite intensity measurements very close to threshold, and thus comparisons to previous results related to this work are of interest. First, the satellite intensities are substantially lower than observed in the high-energy limit ($AlK\alpha$ x rays). Second, measurements by Wuilleumier and Krause¹⁰ for the Ne 2s and 2p levels with fixed-energy photon sources differ markedly from ours in several respects: the photon-energy range, data density, proximity to threshold, and because they studied *valence*-shell photoemission satellites. However, behavior qualitatively similar to our measurements was observed despite those differences. Wuilleumier and Krause plotted their relative satellite intensities against a reduced energy parameter, ϵ/E_0 , where ϵ is the satellite photoelectron kinetic energy and E_0 is the energy required to “promote” a 2p electron from the main ionic-state configuration to form the dominant satellite configuration. For the 2p-photoemission case, E_0 is 34.3 eV. For our 1s-photoemission data, E_0 is ~ 37 –40 eV (Table I). Wuilleumier and Krause observed a constant relative satellite intensity in the high-energy limit, $\epsilon/E_0 \gg 1$, and a decrease in relative intensity for lower values of ϵ/E_0 , which they interpreted as approaching a finite limit for $\epsilon/E_0 \rightarrow 0$, although their lowest measurements fell at $\epsilon/E_0 \approx 2$. Our measurements, in contrast, cover the low-energy range $0.2 \leq \epsilon/E_0 \leq 1.4$. Thus our results extend these studies, for core levels, into a new reduced-energy domain in which the satellite-channel photoelectron is moving more slowly than even the most weakly bound passive electrons. Under these conditions, the wave functions of these passive electrons can better relax to follow the slowly varying atomic potential as the photoelectron leaves, making the sudden approximation invalid.

In the ISCI-FISCI formalism for describing the $Ne^+ 1s2s^22p^5np$ satellite,^{2,3} it can be treated as an eigenstate of the ion, completely equivalent to the “main” peak, and its intensity near threshold is expected to vary with kinetic energy in the same way as that of the main peak, to first approximation. Thus the observed intensity ratio should vary as

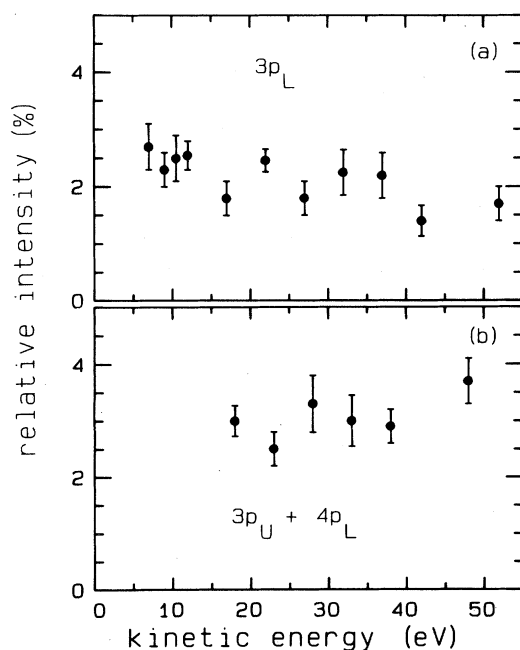


FIG. 2. Intensities of the $3p_L$ satellite (a) and the sum of the satellites $3p_U$ and $4p_L$ (b), relative to the intensity of the 1s main line (= 100), plotted vs satellite kinetic energy.

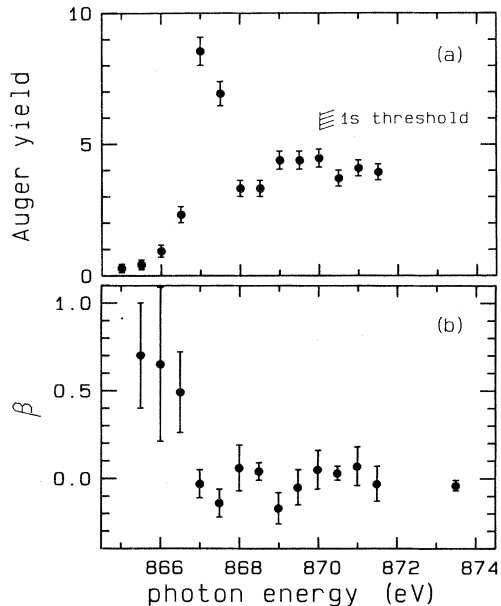


FIG. 3. Yield (a) and asymmetry parameter (b) of the unresolved high-energy peak from Ne vs excitation energy. The unresolved peak contains *KLL*, *KLM*, etc. Auger lines, in addition to valence-shell photoelectrons. Of interest are the two $1s \rightarrow 3p$ resonance emission points at 867.0 and 867.5 eV and the four points above the $\text{Ne}^+(1s)^{-1}$ threshold at 870.2 eV. By setting the mean value of β equal to zero for the points above 870.2 eV to calibrate the spectrometer, $\beta \cong 0$ was determined for the 867.0- and 867.5-eV points. The five points between (with $\beta \cong 0$) arise from several mechanisms, while those for $h\nu < 867$ eV (with $\beta \cong 0.6$) arise mainly from valence photoelectrons.

$$\frac{I_i(h\nu)}{I_0(h\nu)} = C_i \frac{\sigma_0(h\nu - B_i)}{\sigma_0(h\nu - B_0)},$$

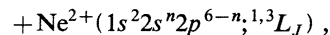
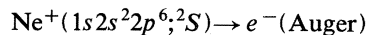
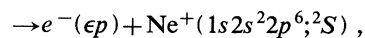
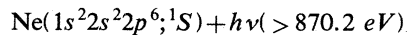
where i labels a particular satellite, 0 labels the main line, C is a constant, and B stands for binding energy. Using the $\text{Ne}(1s)$ cross-section data of Wuilleumier,^{22,23} we would predict the above ratio to be essentially constant throughout our data range. Our results show considerable scatter, but the $3p_L$ intensity appears to be roughly constant with energy, as expected. This tentative conclusion should be confirmed by more accurate measurements.

The MBPT calculation by Ishihara *et al.*¹⁷ of the $3s$ conjugate shakeup satellite shows the intensity decreasing from 5% to 2% between threshold and 50-eV kinetic energy. The calculation also shows that the β parameter changes from -0.3 to $+1.3$ in this energy range. Both of these parameters are required to predict the intensity observed at $\theta = 0^\circ$. The kinetic energy of the $3s$ satellite would be 25 eV for the spectrum shown in Fig. 1. At this energy, the MBPT calculated intensity at $\theta = 0^\circ$ is 2.0%. Satellite $3p_L$ in Fig. 1 has an intensity of 2.5%. We conservatively estimate that the conjugate shakeup satellite must have a relative intensity less than 0.9% in order not to have been observable in this spectrum.

Also present in the neon TOF spectrum was a peak

arising from the unresolved Ne *KLL*, *KLM*, etc. Auger lines. Figure 3(a) shows the intensity of this peak, taken with the 0° detector, plotted versus photon energy near the Ne $1s$ threshold. The photon flux was monitored by the electron yield from a carbon-coated plate in the back of the chamber. The Auger yield curve in Fig. 3(a), measured with a photon-energy bandpass of 0.7 eV, looks quite similar to the absorption spectrum of neon.²¹ The nonzero intensity at $h\nu = 866$ eV and below arises from unresolved valence photoelectrons, with some probable additional contributions from Auger transitions produced by scattered and second-order light. At 867.0 and 867.5 eV, the Auger yield rises sharply because of $1s \rightarrow 3p$ resonance absorption followed by Auger decay or valence autoionization. Additional $1s \rightarrow np$ resonances start at 869.0 eV and lead up to the direct-ionization threshold at 870.2 eV.

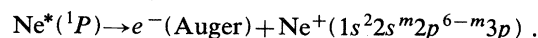
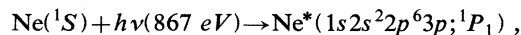
The asymmetry parameter β of the total Auger group was measured as a function of photon energy [Fig. 3(b)]. Above $h\nu = 870.2$ eV, the Auger group arises predominantly from decay of the $1s$ hole state:



$$n = 0, 1, 2.$$

These are the "normal" *KLL* Auger transitions following $1s$ ionization. There are five $^{1,3}L_J$ Auger peaks, all unresolved in our spectra. Because the $\text{Ne}^+(^2S)$ intermediate state is spherically symmetrical, it must be randomly oriented in space. Thus β is required to be identically zero for *each* unresolved component and hence for the total unresolved Auger peak.²⁴ We have used this fact to calibrate the relative efficiency of the two analyzers. Thus β was set equal to zero for the average of the four highest-energy points.

In Fig. 3(a), the two data points at $h\nu = 867.0$ and 867.5 eV arise almost entirely from the $1s \rightarrow 3p$ resonance excitation. Electron spectroscopy studies of analogous inner-shell resonant states in Kr (Ref. 25) and Xe (Ref. 26) show that the resonant states decay predominantly by Auger processes in which the Rydberg electron remains as a spectator. We assume here that similarly the Ne $1s \rightarrow 3p$ resonant state decays primarily by *KLL* Auger transitions in which the $3p$ electron remains as a spectator. Thus the excitation and decay steps are



The resonant Auger electrons are ejected from a $\text{Ne}^*(^1P_1)$ state, so one would expect in principle that they could be produced with anisotropic angular distributions. However, the measured asymmetry parameter of the unresolved resonant Auger group was ~ 0 , which indicates one of the following:

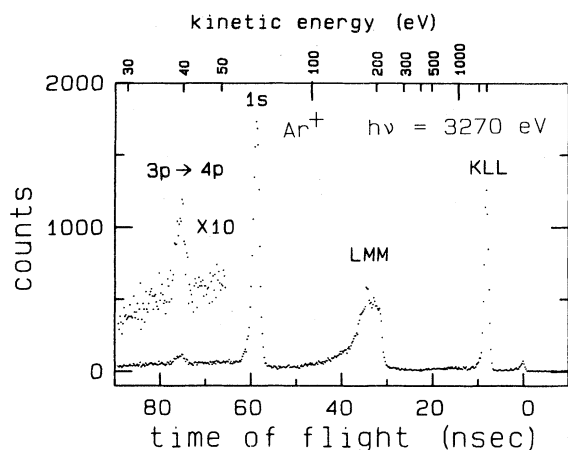


FIG. 4. Electron TOF spectrum of Ar at $h\nu=3270$ eV with a 5-V retarding potential. The accumulation time is 50 min, and there are 4.8 channels per nsec.

(1) $\beta \cong 0$ because nonzero β values for individual Auger transitions average out to zero.

(2) $\beta \cong 0$ because the $3p$ electron acts as a nonparticipating "spectator," essentially decoupled from the core. Hence the Auger electrons are ejected isotropically from the unaligned $\text{Ne}^+(^2S)$ core, as they are above the $1s$ ionization threshold.

High-resolution Auger studies are needed to decide between (1) and (2), and to isolate the valence-electron signal from the Auger electrons. Probably both of these mechanisms contribute to some extent.

Finally, we note that the positive values of β for photon energies below 867 eV are consistent with the expected high-energy behavior of valence-shell photoemission, which accounts for most of the electron intensity in the region $h\nu < 867$ eV.

Figure 4 shows a TOF spectrum of Ar taken at $h\nu=3270$ eV. At 24.6(3) eV above the $1s$ line in binding energy, there is a satellite with 6.0(5)% of the intensity of the main line. The width of the satellite peak in this spectrum is 3 eV FWHM. This satellite can be compared to the $3p^5 4p$ satellite of the Ar $2p$ peak observed by Bristow *et al.*⁷ with Mg $K\alpha$ x rays. The $2p$ satellite is 23.5 eV from the $2p$ main line and has an intensity of 6.0%. This similarity for different core-shell vacancies is predicted by the simple shakeup model.²⁷ Shake-theory calculations of the Ar $1s$ satellite spectrum by Dyllal²⁸ show a $[1s3p]4p(^1S)^2S_{1/2}$ satellite with an excitation energy of 24.4 eV and an intensity of 6.2%. (The square brackets designate the hole configuration.) These calculations also show 0.9% intensity in other satellite peaks at lower binding energies, but within 1 eV. Additional satellites with higher binding energies are calculated at positions over 3 eV from the $3p^5 4p$ peak. Thus Dyllal's predictions of the energy and approximate intensity are confirmed.

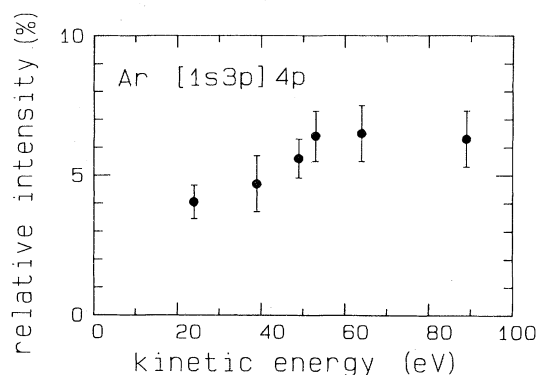


FIG. 5. Variation of the Ar 24.6-eV satellite intensity relative to the main line ($=100$) as a function of satellite kinetic energy. Although the data scatter, the apparent increase is of interest because the data lie in the intermediate range of relative energy ϵ/E_0 between the adiabatic and sudden limits. Taking $E_0=24.6$ eV, the range for these data is $1.0 \leq \epsilon/E_0 \leq 3.6$.

Our measurements of the $[1s3p]4p$ satellite intensity between 23 and 84-eV kinetic energy (Fig. 5) show evidence for increasing relative intensity with increasing energy. This result is of interest because the data range in Fig. 5 lies in the intermediate region of relative energy ϵ/E_0 , between the adiabatic low-energy limit and the sudden high-energy limit. For the Ar $1s$ data, E_0 is 24.6 eV, and the range $1.0 \leq \epsilon/E_0 \leq 3.6$ is covered. Wuilleumier and Krause¹⁰ found strong increases in the relative intensities of the neon valence-shell satellites over a similar range of ϵ/E_0 .

In a complementary experiment, Deslattes *et al.*²⁹ have measured $K\beta$ fluorescence spectra from Ar after excitation with monochromatized photons in the 3163–3606-eV range. They measured the relative intensity of fluorescent radiation from a single $[1s]$ vacancy and from $[1s3p]$ and $[1s3s]$ double vacancies. Each of these three fluorescent peaks may have contributions from Ar neutral, Ar^+ , and Ar^{2+} . The $[1s3p]$ fluorescent intensity is $\sim 30\%$ relative to the $[1s]$ intensity in the energy range of Fig. 5 which, in light of our results, implies that species other than the $[1s3p]4p$ single ion are responsible for most of this intensity.

ACKNOWLEDGMENTS

We thank Z. Hussain for help with the monochromator alignment. This work was supported by the Director, Office of Energy Research, Office of Basic Energy Sciences, Chemical Sciences Division of the U.S. Department of Energy under Contract No. DE-AC03-76SF00098. It was performed at the Stanford Synchrotron Radiation Laboratory, which is supported by the National Science Foundation through the Division of Materials Research. One of us (U.B.) is indebted to the Deutsche Forschungsgemeinschaft (DFG) for financial support.

- *Present address: Department of Chemistry, Pennsylvania State University, University Park, PA 16802.
- †Present address: National Bureau of Standards, Washington, D.C. 20234.
- ‡Present address: Corning Glass Works, Corning, NY 14831.
- §Permanent address: Fachbereich Physik, Technische Universität Berlin, D-1000 Berlin 12, West Germany.
- ¹T. Åberg, *Phys. Rev.* **156**, 35 (1967).
- ²R. L. Martin and D. A. Shirley, *J. Chem. Phys.* **64**, 3685 (1976).
- ³S. T. Manson, *J. Electron Spectrosc.* **9**, 21 (1976).
- ⁴K. G. Dyall and F. P. Larkins, *J. Phys. B* **15**, 203 (1982) and references therein.
- ⁵K. G. Dyall and F. P. Larkins, *J. Phys. B* **15**, 219 (1982).
- ⁶J. D. Talman, G. M. Bancroft, and D. D. Johnston, *Phys. Rev. A* **24**, 669 (1981).
- ⁷D. J. Bristow, J. S. Tse, and G. M. Bancroft, *Phys. Rev. A* **25**, 1 (1982).
- ⁸H. Smid and J. E. Hansen, *J. Phys. B* **14**, L811 (1981).
- ⁹R. L. Martin and D. A. Shirley, *Phys. Rev. A* **13**, 1475 (1976).
- ¹⁰F. Wuilleumier and M. O. Krause, *Phys. Rev. A* **10**, 242 (1974).
- ¹¹M. Y. Adam, F. Wuilleumier, N. Sandner, V. Schmidt, and G. Wendin, *J. Phys. (Paris)* **39**, 129 (1978).
- ¹²M. Y. Adam, F. Wuilleumier, S. Krummacher, V. Schmidt, and W. Mehlhorn, *J. Phys. B* **11**, L413 (1978).
- ¹³D. W. Lindle, T. A. Ferrett, U. Becker, P. H. Kobrin, C. M. Truesdale, H. G. Kerkhoff, and D. A. Shirley (unpublished).
- ¹⁴P. R. Woodruff and J. A. R. Samson, *Phys. Rev. A* **25**, 848 (1982).
- ¹⁵F. P. Larkins, in *Proceedings of the International Conference on X-ray and Atomic Inner-shell Physics, Eugene, Oregon, 1982*, edited by B. Crasemann (American Institute of Physics, New York, 1982).
- ¹⁶H. P. Kelly, *Phys. Rev. A* **6**, 1048 (1972).
- ¹⁷T. Ishihara, J. Mizuno, and T. Watanabe, *Phys. Rev. A* **22**, 1552 (1980); **23**, 2088 (1981).
- ¹⁸U. Gelius, *J. Electron Spectrosc.* **5**, 985 (1974).
- ¹⁹Z. Hussain, E. Umbach, D. A. Shirley, J. Stöhr, and J. Feldhaus, *Nucl. Instrum. Methods* **195**, 115 (1982).
- ²⁰M. G. White, R. A. Rosenberg, G. Gabor, E. D. Poliakoff, G. Thornton, S. H. Southworth, and D. A. Shirley, *Rev. Sci. Instrum.* **50**, 1268 (1979).
- ²¹S. H. Southworth, C. M. Truesdale, P. H. Kobrin, D. W. Lindle, W. D. Brewer, and D. A. Shirley, *J. Chem. Phys.* **76**, 143 (1982).
- ²²F. Wuilleumier, *Adv. X-ray Anal.* **16**, 63 (1973).
- ²³F. Wuilleumier, *J. Phys. (Paris) Colloq.* **32**, C4-88 (1971).
- ²⁴S. Flugge, W. Mehlhorn, and V. Schmidt, *Phys. Rev. Lett.* **29**, 7 (1972).
- ²⁵W. Eberhardt, G. Kalkoffen, and C. Kunz, *Phys. Rev. Lett.* **41**, 156 (1978).
- ²⁶S. Southworth, U. Becker, C. M. Truesdale, P. H. Kobrin, D. W. Lindle, S. Owaki, and D. A. Shirley, *Phys. Rev. A* **28**, 261 (1983).
- ²⁷D. P. Spears, H. J. Fischbeck and T. A. Carlson, *Phys. Rev. A* **9**, 1603 (1974).
- ²⁸K. G. Dyall, *J. Phys. B* **16**, 3137 (1983).
- ²⁹R. D. Deslattes, R. E. LaVilla, P. L. Cowan, and A. Henins, *Phys. Rev. A* **27**, 923 (1983).